ENTROPY STABLE FINITE VOLUME SCHEME FOR IDEAL COMPRESSIBLE MHD ON 2-D CARTESIAN MESHES

PRAVEEN CHANDRASHEKAR[†] AND CHRISTIAN KLINGENBERG[‡]

Abstract. We present a finite volume scheme for ideal compressible magnetohydrodynamic (MHD) equations on 2-D Cartesian meshes. The semi-discrete scheme is constructed to be entropy stable by using the symmetrized version of the equations as introduced by Godunov. We first construct an entropy conservative scheme for which sufficient condition is given and we also derive a numerical flux satisfying this condition. Secondly, following a standard procedure, we make the scheme entropy stable by adding dissipative flux terms using jumps in entropy variables. A semi-discrete high resolution scheme is constructed that preserves the entropy stability of the first order scheme. We demonstrate the robustness of this new scheme on several standard MHD test cases.

Key words. compressible MHD, symmetrization, entropy stability, finite volume scheme

AMS subject classifications.

1. Introduction. The equations of ideal compressible MHD are a system of eight non-linear conservation laws for mass, momentum, energy and magnetic field. Due to their hyperbolic nature, these equations admit discontinuous solutions. The magnetic field has to be divergence-free which is a reflection of the principle that there are no magnetic monopoles. The MHD equations ensure that the rate of change of divergence is zero. If the initial divergence is zero, then it remains zero for future times. In a numerical computation, it is not obvious that the divergence free condition will be satisfied, even approximately. This can lead to instabilities in the computations and/or loss of positivity of density and pressure. Many numerical schemes have been proposed to deal with this important problem starting with the earliest works which were based on one-dimensional Riemann solvers for the 7×7 system of conservation laws [7], [8], [10], [12], [3]. These schemes require additional steps to take care of the zero divergence constraint. In [7] the authors suggest to project the numerical solution obtained for the magnetic field from a 1-D Riemann solver based scheme onto the subspace of zero divergence solutions which involves the solution of an elliptic Poisson equation. Another method is the so-called constrained transport method [12] in which a staggered grid is used to preserve a specific discretization of divergence by solving additional equations for a vector potential $\boldsymbol{A}$ which is related to the magnetic field $\boldsymbol{B}$ by $\boldsymbol{B} = \nabla \times \boldsymbol{A}$. Unstaggered versions of the constrained transport method have also been developed, see [14], [33], [20]. There are many Riemann solvers available in the literature, e.g., based on HLLC schemes [22],[19] or relaxation solvers [6],[23].

A different class of schemes which do not explictly control the divergence are also developed in the literature. Powell [30] noticed that the MHD equations are incompletely hyperbolic and proposed to add source terms to recover the missing eigenvector, leading to a model that is not conservative. A Godunov-type finite volume scheme based on an 8 wave Riemann solver was constructed for the modified equations which lead to a stable scheme without any explicit control on the magnetic divergence. These modified equations have the property that the divergence is advected with the flow. Any numerical errors in the divergence are also expected to be advected thus preventing accumulation of error. While these source terms lead to a

---

[†]TIFR Center for Applicable Mathematics, Bangalore, India (`praveen@tifrbng.res.in`)
[‡]Dept. of Mathematics, Univ. of Würzburg, Würzburg, Germany (`klingenberg@mathematik.uni-wuerzburg.de`)

stable scheme in computations, it is known that in some problems, the non conservative nature of the scheme leads to wrong solutions [39]. The generalization of this approach in [11] involved adding additional source terms which diffuse the error in divergence apart from advecting it and requires solution of an extra scalar equation. In the framework of relaxation solvers [23], source terms are added only in the magnetic field equation which helps to construct a positivity preserving scheme. Much before this, Godunov [18] had pointed out that systems like MHD which have a divergence constraint cannot be symmetrized unless some additional source terms are added. These source terms are identical to those developed by Powell. The ability to symmetrize the equations implies the existence of an entropy condition which gives some stability to the solutions.

The above approaches have been used to develop high order schemes following different techniques. High order schemes based on TVD reconstruction, ENO and WENO reconstructions, ADER-WENO scheme, etc., are also available, see e.g., [28],[38],[1],[2]. Discontinuous Galerkin schemes for MHD have been developed, see [25], [26] for central DG schemes, and [4], [5] for entropy stable schemes.

In this work we develop a semi-discrete entropy stable finite volume scheme for MHD equations on 2-D Cartesian meshes, and the scheme can be easily extended to three dimensions. Our approach which uses colocated variables for all the variables, is based on the following ingredients where the main design principle is to obtain an entropy stable scheme.

1. We construct an entropy conservative scheme for MHD equations in Godunov's symmetrized form. For this purpose we give sufficient conditions on the numerical fluxes and give one example of a flux that satisfies this condition

2. We then add dissipative fluxes which lead to entropy production and hence entropy stability. A high order version of the scheme is constructed using reconstruction scheme that is also entropy stable.

3. The semi-discrete equations resulting from the above steps are integrated in time using a Runge-Kutta scheme.

The above approach has already been used for standard conservation laws like Euler equations starting with [36],[37] where entropy conservative and entropy stable schemes were characterized. Practical numerical flux functions that satisfy necessary conditions for entropy conservation were later developed in [21],[9]. Entropy stable dissipation operators have been developed in [37] and also used in [21],[15],[9]. The high resolution scheme used in the present work is similar to the TeCNO scheme [15] developed in the context of usual conservation laws where the high order entropy conservative scheme from [24] is used. The important idea in this scheme is to ensure that the jump in the reconstructed quantities at any cell face must have the same sign as the jump in the quantities at the cell centers. This *sign property* enables us to obtain the desired entropy inequalities. Arbitrarily high order sign preserving ENO reconstructions have been presented in [15] though in the present work, we only discuss the second order version.

The resulting semi-discrete scheme is entropy stable and a fully discrete scheme is obtained by using a Runge-Kutta scheme for time integration. Similar to the TeCNO schemes, the fully discrete scheme presented here cannot be proven to be entropy stable but we show through numerical experiments, that entropy is generated by the fully discrete scheme thus indicating stability of the numerical scheme. The numerical examples given in this paper show that the proposed scheme is stable without any explicit control on the divergence. However on some test problems, it is found to

give wrong solutions, which is a common problem of all non-conservative schemes as pointed out in [39]. A natural resolution to this problem is provided by the use of a space-time discontinuous Galerkin (DG) framework which is part of our ongoing work. The numerical flux developed in this paper provides the necessary ingredients to construct an entropy stable DG scheme. The source terms can be avoided by the use of locally divergence-free basis functions for the magnetic field and hence the scheme will be conservative, though requiring additional stabilization terms[*].

The rest of the paper is organized as follows. In section 2 we introduce the MHD equations and discuss its symmetrization properties and Godunov's modification. In section 3 we present the finite volume scheme, and discuss the entropy conservative and entropy stable schemes, together with the high resolution version of the scheme. Section 4 presents the results of some standard MHD test cases computed with the present scheme. The paper ends with summary and conclusions in section 5.

2. Ideal MHD equations. The equations governing compressible ideal MHD flows can be written as a system of conservation laws for mass, momentum, energy and magnetic field in the following form

$$\frac{\partial \rho}{\partial t} + \nabla \cdot (\rho \boldsymbol{u}) = 0$$

$$\frac{\partial (\rho \boldsymbol{u})}{\partial t} + \nabla \cdot [\rho \boldsymbol{u}\boldsymbol{u} + (p + \frac{1}{2}|\boldsymbol{B}|^2)I - \boldsymbol{B}\boldsymbol{B}] = 0$$

$$\frac{\partial E}{\partial t} + \nabla \cdot [(E + p + \frac{1}{2}|\boldsymbol{B}|^2)\boldsymbol{u} - (\boldsymbol{u} \cdot \boldsymbol{B})\boldsymbol{B}] = 0$$

$$\frac{\partial \boldsymbol{B}}{\partial t} + \nabla \cdot (\boldsymbol{u}\boldsymbol{B} - \boldsymbol{B}\boldsymbol{u}) = 0$$

where ρ is the density, $\boldsymbol{u}$ is the fluid velocity, p is the pressure, E is the total energy and $\boldsymbol{B}$ is the magnetic field. We assume that the total energy E is given by

$$E = \frac{p}{\gamma - 1} + \frac{1}{2}\rho|\boldsymbol{u}|^2 + \frac{1}{2}|\boldsymbol{B}|^2$$

where $\gamma > 1$ is the ratio of specific heats which is taken to be constant. The ideal MHD equations form a system of hyperbolic conservation laws which we will write in component form as

(2.1)
$$\frac{\partial \boldsymbol{w}}{\partial t} + \frac{\partial \boldsymbol{f}_\alpha}{\partial x_\alpha} = 0$$

We use the Einstein summation convention on repeated indices like α which runs over the number of spatial dimensions. In the two dimensional case, the expressions for $\boldsymbol{w}$, $\boldsymbol{f}_\alpha$ are given by

$$\boldsymbol{w} = \begin{bmatrix} \rho, & \rho u_1, & \rho u_2, & \rho u_3, & E, & B_1, & B_2, & B_3 \end{bmatrix}^\top$$

---

[*]Tim Barth, private communication

$$
\boldsymbol{f}_1 = \begin{bmatrix} \rho u_1 \\ p + \rho u_1^2 + \frac{1}{2}|\boldsymbol{B}|^2 - B_1^2 \\ \rho u_1 u_2 - B_1 B_2 \\ \rho u_1 u_3 - B_1 B_3 \\ (E + p + \frac{1}{2}|\boldsymbol{B}|^2)u_1 - (\boldsymbol{u} \cdot \boldsymbol{B})B_1 \\ 0 \\ u_1 B_2 - u_2 B_1 \\ u_1 B_3 - u_3 B_1 \end{bmatrix}, \quad
\boldsymbol{f}_2 = \begin{bmatrix} \rho u_2 \\ \rho u_1 u_2 - B_1 B_2 \\ p + \rho u_2^2 + \frac{1}{2}|\boldsymbol{B}|^2 - B_2^2 \\ \rho u_2 u_3 - B_2 B_3 \\ (E + p + \frac{1}{2}|\boldsymbol{B}|^2)u_2 - (\boldsymbol{u} \cdot \boldsymbol{B})B_2 \\ u_2 B_1 - u_1 B_2 \\ 0 \\ u_2 B_3 - u_3 B_2 \end{bmatrix}
$$

Note that we include the velocity and magnetic field components in the third direction but these are assumed to be independent of the third spatial dimension. An additional constraint that needs to be satisfied is that the magnetic field $\boldsymbol{B}$ must be divergence-free,

$$
\nabla \cdot \boldsymbol{B} = 0
$$

In fact if the above constraint is satisfied at the initial time, then the equation for $\boldsymbol{B}$ implies that

$$
\frac{\partial}{\partial t} \nabla \cdot \boldsymbol{B} = 0
$$

and the constraint is satisfied for future times also. In general we have to interpret the solution in the distributional sense, see e.g. [13]. If $\boldsymbol{B}$ is discontinuous across some surface, then the divergence condition implies that the normal component of $\boldsymbol{B}$ is continuous across the surface of discontinuity.

2.1. Symmetric form and entropy variables. It is well known that weak solutions of conservations laws are not unique. According to the second law of thermodynamics, the entropy condition is an important property which must be satisfied by any physical system. By demanding that weak solutions satisfy some form of the entropy condition, we can obtain uniqueness, atleast for scalar problems [27], while for systems this question is still open in general. However, the entropy condition is still a useful design principle since in most cases, it is the only non-linear stability property we can prove for numerical schemes. One way to introduce the entropy condition is through a convex entropy function.

DEFINITION 1. *A strictly convex function $U(\boldsymbol{w})$ is called an* **entropy** *for the system (2.1) if there are associated* **entropy fluxes** $F_\alpha(\boldsymbol{w})$ *such that*

(2.2) $$
F'_\alpha(\boldsymbol{w}) = U'(\boldsymbol{w})\boldsymbol{f}'_\alpha(\boldsymbol{w})
$$

The functions (U, F_α) are said to form an *entropy pair*. If a system of conservation laws admits an entropy pair, then smooth solutions of the conservation law satisfy an additional entropy conservation law as can be seen below

$$
0 = U'(\boldsymbol{w})\frac{\partial \boldsymbol{w}}{\partial t} + U'(\boldsymbol{w})\boldsymbol{f}'_\alpha(\boldsymbol{w})\frac{\partial \boldsymbol{w}}{\partial x_\alpha} = \frac{\partial U}{\partial t} + \frac{\partial F_\alpha}{\partial x_\alpha}
$$

For solutions which are not smooth, the above equation is replaced with an inequality

$$
\frac{\partial U}{\partial t} + \frac{\partial F_\alpha}{\partial x_\alpha} \le 0
$$

which is to be interpreted in the weak sense and is known as the entropy condition.

DEFINITION 2. *The conservation law (2.1) is said to be symmetrizable if there exists a change of variables $\boldsymbol{w} \to \boldsymbol{v}$ which symmetrizes it, i.e., equation (2.1) becomes*

$$\frac{\partial \boldsymbol{w}}{\partial \boldsymbol{v}} \frac{\partial \boldsymbol{v}}{\partial t} + \frac{\partial \boldsymbol{f}_\alpha}{\partial \boldsymbol{w}} \frac{\partial \boldsymbol{w}}{\partial \boldsymbol{v}} \frac{\partial \boldsymbol{v}}{\partial x_\alpha} = 0$$

where $\frac{\partial \boldsymbol{w}}{\partial \boldsymbol{v}}$ is a symmetric positive definite matrix and $\frac{\partial \boldsymbol{f}_\alpha}{\partial \boldsymbol{w}} \frac{\partial \boldsymbol{w}}{\partial \boldsymbol{v}}$ are symmetric matrices.

There is a close connection between the existence of an entropy pair and the symmetrization of a system of conservation laws.

THEOREM 2.1. *(Mock) A necessary and sufficient condition for the system (2.1) to possess a strictly convex entropy $U(\boldsymbol{w})$ is that there exists a change of dependent variables $\boldsymbol{w} = \boldsymbol{w}(\boldsymbol{v})$ that symmetrizes (2.1). (For proof, see [17])*

If the transformation $\boldsymbol{w} \to \boldsymbol{v}$ symmetrizes the equations, then there exist twice differentiable functions $\mathcal{U}(\boldsymbol{v})$, $\mathcal{F}_\alpha(\boldsymbol{v})$ with $\mathcal{U}(\boldsymbol{v})$ strictly convex such that

$$\boldsymbol{w} = \mathcal{U}'(\boldsymbol{v})^\top, \qquad \boldsymbol{f}_\alpha = \mathcal{F}_\alpha'(\boldsymbol{v})^\top$$

Define $U(\boldsymbol{w})$ to be the Legendre transform of $\mathcal{U}(\boldsymbol{v})$

$$U(\boldsymbol{w}) = \sup_{\boldsymbol{v}} \{\boldsymbol{v} \cdot \boldsymbol{w} - \mathcal{U}(\boldsymbol{v})\}$$

Let the supremum be attained at $\boldsymbol{v}^* = \boldsymbol{v}(\boldsymbol{w})$ so that

$$(2.3) \qquad U(\boldsymbol{w}) = \boldsymbol{v}(\boldsymbol{w}) \cdot \boldsymbol{w} - \mathcal{U}(\boldsymbol{v}(\boldsymbol{w}))$$

Differentiating this expression we get

$$U'(\boldsymbol{w})^\top = \boldsymbol{v}(\boldsymbol{w}) + \boldsymbol{v}'(\boldsymbol{w})\boldsymbol{w} - \boldsymbol{v}'(\boldsymbol{w})\mathcal{U}'(\boldsymbol{v}(\boldsymbol{w}))^\top = \boldsymbol{v}$$

Let us also define

$$(2.4) \qquad F_\alpha(\boldsymbol{w}) = \boldsymbol{v}(\boldsymbol{w}) \cdot \boldsymbol{f}_\alpha(\boldsymbol{w}) - \mathcal{F}_\alpha(\boldsymbol{v}(\boldsymbol{w}))$$

Differentiating this expression

$$F_\alpha'(\boldsymbol{w}) = \boldsymbol{v}(\boldsymbol{w}) \cdot \boldsymbol{f}_\alpha'(\boldsymbol{w}) + \boldsymbol{v}'(\boldsymbol{w})\boldsymbol{f}_\alpha - \boldsymbol{v}'(\boldsymbol{w})\mathcal{F}_\alpha'(\boldsymbol{v})^\top = \boldsymbol{v}(\boldsymbol{w}) \cdot \boldsymbol{f}_\alpha'(\boldsymbol{w}) = U'(\boldsymbol{w})\boldsymbol{f}_\alpha(\boldsymbol{w})$$

Thus (2.3), (2.4) give the relationship between the entropy pair (U, F_α) and the conjugate quantities $(\mathcal{U}, \mathcal{F}_\alpha)$.

2.2. Entropy function for ideal MHD. We would like to ask if the MHD equations have an entropy function and if they are symmetrizable. If we define the thermodynamic entropy

$$s = \ln(p\rho^{-\gamma})$$

then the equations of ideal MHD can be used to derive an equation for ρs

$$\frac{\partial(\rho s)}{\partial t} + \nabla \cdot (\rho s \boldsymbol{u}) + (\gamma - 1)\frac{\rho(\boldsymbol{u} \cdot \boldsymbol{B})}{p}\nabla \cdot \boldsymbol{B} = 0$$

This equation suggests that under the constraint $\nabla \cdot \boldsymbol{B} = 0$, the following quantities

$$(2.5) \qquad U = -\frac{\rho s}{\gamma - 1}, \qquad F_\alpha = -\frac{\rho s u_\alpha}{\gamma - 1}$$

satisfy an additional conservation law for smooth solutions, so that U is an entropy function. The entropy variables corresponding to the above entropy function are given by

$$\boldsymbol{v} = U'(\boldsymbol{w})^\top = \left[\tfrac{\gamma - s}{\gamma - 1} - \beta|\boldsymbol{u}|^2, \quad 2\beta\boldsymbol{u}, \quad -2\beta, \quad 2\beta\boldsymbol{B} \right]^\top, \qquad \text{where} \qquad \beta = \frac{\rho}{2p}$$

However the change of variable $\boldsymbol{w} \to \boldsymbol{v}$ fails to symmetrize the ideal MHD equations [4], i.e.,

$$\frac{\partial \boldsymbol{f}_\alpha}{\partial \boldsymbol{v}} \neq \left(\frac{\partial \boldsymbol{f}_\alpha}{\partial \boldsymbol{v}} \right)^\top$$

Moreover, (U, F_α) do not satisfy equation (2.2); instead we have

(2.6) $$F'_\alpha(\boldsymbol{w}) = U'(\boldsymbol{w})\boldsymbol{f}'_\alpha(\boldsymbol{w}) + 2\beta(\boldsymbol{u} \cdot \boldsymbol{B})B'_\alpha(\boldsymbol{w})$$

2.3. Godunov's symmetrization of ideal MHD equations. To achieve symmetrization of systems with divergence constraint like ideal MHD, Godunov [18, 5] introduced a modified form of the ideal MHD equations. Here, we largely follow the approach in [4, 5]. In terms of the symmetrization variables $\boldsymbol{v}$ let $\phi(\boldsymbol{v})$ be a homogeneous function of degree one, i.e.,

(2.7) $$\boldsymbol{v} \cdot \phi'(\boldsymbol{v})^\top = \phi(\boldsymbol{v})$$

Then consider the modified MHD equations

(2.8) $$\frac{\partial \boldsymbol{w}}{\partial t} + \frac{\partial \boldsymbol{f}_\alpha}{\partial x_\alpha} + \phi'(\boldsymbol{v})^\top \nabla \cdot \boldsymbol{B} = 0$$

Since $\nabla \cdot \boldsymbol{B} = 0$ the above modification is consistent. If the transformation $\boldsymbol{w} \to \boldsymbol{v}$ symmetrizes equation (2.8), then there exist twice differentiable functions $\mathcal{U}(\boldsymbol{v}), \mathcal{F}_\alpha(\boldsymbol{v})$ with $\mathcal{U}(\boldsymbol{v})$ strictly convex such that

(2.9) $$\boldsymbol{w} = \mathcal{U}'(\boldsymbol{v})^\top, \qquad \boldsymbol{f}_\alpha = \mathcal{F}'_\alpha(\boldsymbol{v})^\top - \phi'(\boldsymbol{v})^\top B_\alpha$$

We can see that this is true by combining (2.8), (2.9) to obtain

$$\underbrace{\mathcal{U}''(\boldsymbol{v})}_{SPD} \frac{\partial \boldsymbol{v}}{\partial t} + \underbrace{(\mathcal{F}''_\alpha(\boldsymbol{v}) - \phi''(\boldsymbol{v})B_\alpha)}_{Sym} \frac{\partial \boldsymbol{v}}{\partial x_\alpha} = 0$$

which is in symmetric form. Now define U and F_α as

(2.10) $$U(\boldsymbol{w}) = \boldsymbol{v}(\boldsymbol{w}) \cdot \boldsymbol{w} - \mathcal{U}(\boldsymbol{v}(\boldsymbol{w})), \qquad F_\alpha(\boldsymbol{w}) = \boldsymbol{v}(\boldsymbol{w}) \cdot \mathcal{F}'_\alpha(\boldsymbol{v}(\boldsymbol{w})) - \mathcal{F}_\alpha(\boldsymbol{v}(\boldsymbol{w}))$$

Differentiating $U(\boldsymbol{w}), F_\alpha(\boldsymbol{w})$, we obtain $\boldsymbol{v} = U'(\boldsymbol{w})^\top$ and

(2.11) $$F'_\alpha(\boldsymbol{w}) = \boldsymbol{v}(\boldsymbol{w}) \cdot \boldsymbol{f}'_\alpha(\boldsymbol{w}) + \phi(\boldsymbol{v})B'_\alpha(\boldsymbol{w}) = U'(\boldsymbol{w})\boldsymbol{f}'_\alpha(\boldsymbol{w}) + \phi(\boldsymbol{v})B'_\alpha(\boldsymbol{w})$$

Now taking dot product of entropy variables $\boldsymbol{v}$ with (2.8)

$$\begin{aligned}
0 &= \boldsymbol{v} \cdot \left(\frac{\partial \boldsymbol{w}}{\partial t} + \frac{\partial \boldsymbol{f}_\alpha}{\partial x_\alpha} + \phi'(\boldsymbol{v})^\top \nabla \cdot \boldsymbol{B} \right) \\
&= \frac{\partial U}{\partial t} + \left(\boldsymbol{v} \cdot \frac{\partial \boldsymbol{f}_\alpha}{\partial \boldsymbol{w}} + \phi(\boldsymbol{v})B'_\alpha(\boldsymbol{w}) \right) \frac{\partial \boldsymbol{w}}{\partial x_\alpha} \\
&= \frac{\partial U}{\partial t} + \frac{\partial F_\alpha}{\partial \boldsymbol{w}} \frac{\partial \boldsymbol{w}}{\partial x_\alpha}, \qquad \text{using (2.11)} \\
&= \frac{\partial U}{\partial t} + \frac{\partial F_\alpha}{\partial x_\alpha}
\end{aligned}$$

We thus obtain the entropy equation without having to make use of the zero divergence condition. This will be useful in constructing stable numerical scheme, where the numerical divergence may not be zero.

We have to still find an entropy pair (U, F_α). Taking the entropy and entropy flux as in (2.5), we can determine the function $\phi(v)$ by comparing (2.11) with (2.6)

$$(2.12) \qquad\qquad \phi(v) = 2\beta(u \cdot B)$$

In terms of the components of v, this function can be written as

$$\phi(v) = -\frac{v_2 v_6 + v_3 v_7 + v_4 v_8}{v_5}$$

which is homogeneous of degree one. Moreover, computing its Jacobian we obtain

$$\phi'(v) = \begin{bmatrix} 0, & B, & u \cdot B, & u \end{bmatrix}$$

With the above choice of $\phi(v)$ the MHD equations (2.8) are identical to the equations proposed by Powell [30] using different considerations. From (2.7), (2.9), (2.10) the entropy flux is

$$(2.13) \qquad\qquad F_\alpha = v \cdot f_\alpha + \phi B_\alpha - \mathcal{F}_\alpha$$

while the conjugate variables are given by

$$\mathcal{U} = v \cdot w - U = \rho + \beta|B|^2$$

and

$$\mathcal{F}_\alpha = v \cdot f_\alpha + \phi B_\alpha - F_\alpha = \rho u_\alpha + \beta u_\alpha |B|^2 = \mathcal{U} u_\alpha$$

2.4. Induction equation. In the modified MHD system (2.8), the induction equation is given by

$$\frac{\partial B}{\partial t} + \nabla \cdot (uB - Bu) + u\nabla \cdot B = 0$$

Define $\mathcal{D} = \nabla \cdot B$ and taking divergence of above equation we get

$$\frac{\partial \mathcal{D}}{\partial t} + \nabla \cdot (u\mathcal{D}) = 0$$

Using the continuity equation we can rewrite this equation as

$$\frac{\partial}{\partial t}\left(\frac{\mathcal{D}}{\rho}\right) + u \cdot \nabla\left(\frac{\mathcal{D}}{\rho}\right) = 0$$

The quantity $\frac{\mathcal{D}}{\rho}$ is constant along particle paths. If the initial value of $\mathcal{D}$ is zero, then it remains zero for later times. If the fluid entering the domain has zero divergence, then the divergence is zero throughout the domain. This property may be useful in computations since the errors in divergence may be advected away by the flow [30] instead of accumulating in some region and causing instabilities.

3. Finite volume method. We now construct a finite volume scheme for equation (2.8). Consider a uniform Cartesian mesh with spacing Δx, Δy. The cell centers are indexed by (i,j) while the faces are indexed by half indices. E.g., the face between (i,j) and $(i+1,j)$ is denoted by $(i+\frac{1}{2},j)$, etc. Let us define the following notations for the arithmetic average of any quantity

$$\overline{(\cdot)}_{i+\frac{1}{2},j} = \frac{1}{2}[(\cdot)_{i,j} + (\cdot)_{i+1,j}], \qquad \overline{(\cdot)}_{i,j+\frac{1}{2}} = \frac{1}{2}[(\cdot)_{i,j} + (\cdot)_{i,j+1}]$$

The semi-discrete finite volume scheme for (2.8) is given by

$$
\begin{aligned}
\frac{\mathrm{d}}{\mathrm{d}t}\boldsymbol{w}_{i,j} &+ \frac{\boldsymbol{f}_{1,i+\frac{1}{2},j} - \boldsymbol{f}_{1,i-\frac{1}{2},j}}{\Delta x} + \frac{\boldsymbol{f}_{2,i,j+\frac{1}{2}} - \boldsymbol{f}_{2,i,j-\frac{1}{2}}}{\Delta y} \\
&+ \phi'(\boldsymbol{v}_{i,j})^{\top}\left(\frac{\overline{B}_{1,i+\frac{1}{2},j} - \overline{B}_{1,i-\frac{1}{2},j}}{\Delta x} + \frac{\overline{B}_{2,i,j+\frac{1}{2}} - \overline{B}_{2,i,j-\frac{1}{2}}}{\Delta y}\right) = 0
\end{aligned}
$$

(3.1)

The quantities $\boldsymbol{f}_{1,i+\frac{1}{2},j}$, $\boldsymbol{f}_{2,i,j+\frac{1}{2}}$ are numerical fluxes in the x, y directions across the vertical and horizontal faces of the cells, respectively. The divergence of the magnetic field in the source term has been discretized using central differencing. We have to next specify how the numerical fluxes are computed. In the first step, we construct an entropy conservative scheme followed by an entropy stable scheme.

3.1. Entropy conservative scheme. For usual symmetrizable conservation laws like Euler equations, there is a theory of entropy conservative schemes, see e.g., [37]. However this is not sufficient in the case of MHD, see the remark after the following theorem. For the MHD equations, the next theorem gives sufficient conditions on the numerical flux so that the scheme given by (3.1) is entropy conservative.

THEOREM 3.1. *Assume that the numerical fluxes $\boldsymbol{f}_{1,i+\frac{1}{2},j}$, $\boldsymbol{f}_{2,i,j+\frac{1}{2}}$ satisfy*

(3.2) $$(\boldsymbol{v}_{i+1,j} - \boldsymbol{v}_{i,j}) \cdot \boldsymbol{f}_{1,i+\frac{1}{2},j} = \mathcal{F}_{1,i+1,j} - \mathcal{F}_{1,i,j} - (\phi_{i+1,j} - \phi_{i,j})\overline{B}_{1,i+\frac{1}{2},j}$$

(3.3) $$(\boldsymbol{v}_{i,j+1} - \boldsymbol{v}_{i,j}) \cdot \boldsymbol{f}_{2,i,j+\frac{1}{2}} = \mathcal{F}_{2,i,j+1} - \mathcal{F}_{2,i,j} - (\phi_{i,j+1} - \phi_{i,j})\overline{B}_{2,i,j+\frac{1}{2}}$$

Then the semi-discrete finite volume scheme (3.1) is entropy conservative, i.e., it satisfies

(3.4) $$\frac{d}{dt}U(\boldsymbol{w}_{i,j}) + \frac{F_{1,i+\frac{1}{2},j} - F_{1,i-\frac{1}{2},j}}{\Delta x} + \frac{F_{2,i,j+\frac{1}{2}} - F_{2,i,j-\frac{1}{2}}}{\Delta y} = 0$$

where the numerical entropy fluxes are given by

(3.5) $$F_{1,i+\frac{1}{2},j} = \overline{\boldsymbol{v}}_{i+\frac{1}{2},j} \cdot \boldsymbol{f}_{1,i+\frac{1}{2},j} + \overline{\phi}_{i+\frac{1}{2},j}\overline{B}_{1,i+\frac{1}{2},j} - \overline{\mathcal{F}}_{1,i+\frac{1}{2},j}$$

(3.6) $$F_{2,i,j+\frac{1}{2}} = \overline{\boldsymbol{v}}_{i,j+\frac{1}{2}} \cdot \boldsymbol{f}_{2,i,j+\frac{1}{2}} + \overline{\phi}_{i,j+\frac{1}{2}}\overline{B}_{2,i,j+\frac{1}{2}} - \overline{\mathcal{F}}_{2,i,j+\frac{1}{2}}$$

Proof: First of all, we can easily check that the above numerical entropy fluxes are consistent with the entropy flux as given in equation (2.13). Taking dot product of $\boldsymbol{v}_{i,j}$ with the finite volume scheme (3.1) yields equation (3.4). We can verify this result by a reverse calculation as follows. First of all

$$
\begin{aligned}
F_{1,i+\frac{1}{2},j} - F_{1,i-\frac{1}{2},j} = &\ \overline{\boldsymbol{v}}_{i+\frac{1}{2},j} \cdot \boldsymbol{f}_{1,i+\frac{1}{2},j} - \overline{\boldsymbol{v}}_{i-\frac{1}{2},j} \cdot \boldsymbol{f}_{1,i-\frac{1}{2},j} \\
&+ \overline{\phi}_{i+\frac{1}{2},j}\overline{B}_{1,i+\frac{1}{2},j} - \overline{\phi}_{i-\frac{1}{2},j}\overline{B}_{1,i-\frac{1}{2},j} \\
&- (\overline{\mathcal{F}}_{1,i+\frac{1}{2},j} - \overline{\mathcal{F}}_{1,i-\frac{1}{2},j})
\end{aligned}
$$

Using (3.2) we get

$$
\begin{aligned}
\overline{\mathcal{F}}_{1,i+\frac{1}{2},j} - \overline{\mathcal{F}}_{1,i-\frac{1}{2},j} &= \frac{1}{2}(\mathcal{F}_{1,i+1,j} - \mathcal{F}_{1,i,j}) + \frac{1}{2}(\mathcal{F}_{1,i,j} - \mathcal{F}_{1,i-1,j}) \\
&= \frac{1}{2}[(\boldsymbol{v}_{i+1,j} - \boldsymbol{v}_{i,j})\cdot\boldsymbol{f}_{1,i+\frac{1}{2},j} + (\phi_{i+1,j} - \phi_{i,j})\overline{B}_{1,i+\frac{1}{2},j}] \\
&\quad + \frac{1}{2}[(\boldsymbol{v}_{i,j} - \boldsymbol{v}_{i-1,j})\cdot\boldsymbol{f}_{1,i-\frac{1}{2},j} + (\phi_{i,j} - \phi_{i-1,j})\overline{B}_{1,i-\frac{1}{2},j}]
\end{aligned}
$$

and hence

$$
\begin{aligned}
F_{1,i+\frac{1}{2},j} - F_{1,i-\frac{1}{2},j} &= \boldsymbol{v}_{i,j}\cdot(\boldsymbol{f}_{1,i+\frac{1}{2},j} - \boldsymbol{f}_{1,i-\frac{1}{2},j}) + \phi_{i,j}(\overline{B}_{1,i+\frac{1}{2},j} - \overline{B}_{1,i-\frac{1}{2},j}) \\
&= \boldsymbol{v}_{i,j}\cdot\left[(\boldsymbol{f}_{1,i+\frac{1}{2},j} - \boldsymbol{f}_{1,i-\frac{1}{2},j}) + \phi'(\boldsymbol{v}_{i,j})^\top(\overline{B}_{1,i+\frac{1}{2},j} - \overline{B}_{1,i-\frac{1}{2},j})\right]
\end{aligned}
$$

where we made use of (2.7). Similarly it is easy to show that

$$
F_{2,i,j+\frac{1}{2}} - F_{2,i,j-\frac{1}{2}} = \boldsymbol{v}_{i,j}\cdot\left[(\boldsymbol{f}_{2,i,j+\frac{1}{2}} - \boldsymbol{f}_{2,i,j-\frac{1}{2}}) + \phi'(\boldsymbol{v}_{i,j})^\top(\overline{B}_{2,i,j+\frac{1}{2}} - \overline{B}_{2,i,j-\frac{1}{2}})\right]
$$

This completes the proof of the theorem.

Remark. The definition of entropy conservative flux given in (3.2), (3.3) seems to be essential. If we adopt the standard definition of Tadmor [37] and require that the numerical flux satisfy the following condition

(3.7) $$\qquad\qquad (\boldsymbol{v}_{i+1,j} - \boldsymbol{v}_{i,j})\cdot\boldsymbol{f}_{1,i+\frac{1}{2},j} = \mathcal{F}_{1,i+1,j} - \mathcal{F}_{1,i,j}$$

then

$$
\begin{aligned}
&\boldsymbol{v}_{i,j}\cdot\left[(\boldsymbol{f}_{1,i+\frac{1}{2},j} - \boldsymbol{f}_{1,i-\frac{1}{2},j}) + \phi'(\boldsymbol{v}_{i,j})^\top\frac{B_{1,i+1,j} - B_{1,i-1,j}}{2}\right] \\
&= \left(\overline{\boldsymbol{v}}_{i+\frac{1}{2},j}\cdot\boldsymbol{f}_{1,i+\frac{1}{2},j} + \phi_{i,j}\overline{B}_{1,i+\frac{1}{2},j} - \overline{\mathcal{F}}_{1,i+\frac{1}{2},j}\right) \\
&\quad - \left(\overline{\boldsymbol{v}}_{i-\frac{1}{2},j}\cdot\boldsymbol{f}_{1,i-\frac{1}{2},j} + \phi_{i,j}\overline{B}_{1,i-\frac{1}{2},j} - \overline{\mathcal{F}}_{1,i-\frac{1}{2},j}\right)
\end{aligned}
$$

But the above quantities inside the brackets are not fluxes due to the presence of the term $\phi_{i,j}$ and we cannot obtain a discrete entropy equation. Moreover, we are not able to find consistent numerical fluxes which satisfy equation (3.7). Finally, from equation (2.9) we obtain

$$
\frac{\partial\boldsymbol{v}}{\partial x_1}\cdot\boldsymbol{f}_1 = \frac{\partial\mathcal{F}_1}{\partial x_1} - \frac{\partial\phi}{\partial x_1}B_1
$$

and (3.2) is a discrete approximation of the above equation. Thus the usual necessary conditions as in [37] need to be modfied for the MHD system to account for the divergence constraint.

3.2. Construction of entropy conservative fluxes. We now want to construct explicit and simple expressions for numerical fluxes satisfying equation (3.2) and (3.3). Consider equation (3.2) which we will write without any grid indices as

(3.8) $$\qquad\qquad \Delta\boldsymbol{v}\cdot\boldsymbol{f}_1 = \Delta\mathcal{F}_1 - \overline{B}_1\Delta\phi$$

and the overbar denotes the arithmetic average. Following Roe [32], let us introduce the logarithmic average $\hat{\varphi}$ of two strictly positive quantities φ_l, φ_r as

$$\hat{\varphi} = \frac{\varphi_r - \varphi_l}{\ln \varphi_r - \ln \varphi_l} = \frac{\Delta \varphi}{\Delta \ln \varphi}$$

A numerically stable procedure to compute the average when $\varphi_l \approx \varphi_r$ is given in [21]. We will also need the following formula for the difference of a product of two quantities

$$\Delta(ab) = \bar{b}\Delta a + \bar{a}\Delta b$$

Following the approach in [9], we write the difference in entropy variables in terms of the differences in ρ, u_1, u_2, u_3, β, B_1, B_2, B_3 as

$$\Delta \boldsymbol{v} = \begin{bmatrix} \frac{1}{\bar{\rho}}\Delta\rho - 2\bar{\beta}(\bar{u}_1\Delta u_1 + \bar{u}_2\Delta u_2 + \bar{u}_3\Delta u_3) + \left[\frac{1}{(\gamma-1)\hat{\beta}} - \overline{|\boldsymbol{u}|^2}\right]\Delta\beta \\ 2\bar{\beta}\Delta u_1 + 2\bar{u}_1\Delta\beta \\ 2\bar{\beta}\Delta u_2 + 2\bar{u}_2\Delta\beta \\ 2\bar{\beta}\Delta u_3 + 2\bar{u}_3\Delta\beta \\ -2\Delta\beta \\ 2\bar{\beta}\Delta B_1 + 2\bar{B}_1\Delta\beta \\ 2\bar{\beta}\Delta B_2 + 2\bar{B}_2\Delta\beta \\ 2\bar{\beta}\Delta B_3 + 2\bar{B}_3\Delta\beta \end{bmatrix}, \quad \boldsymbol{f}_1 = \begin{bmatrix} f_1^{(1)} \\ f_1^{(2)} \\ f_1^{(3)} \\ f_1^{(4)} \\ f_1^{(5)} \\ f_1^{(6)} \\ f^{(7)} \\ f^{(8)} \end{bmatrix}$$

where the superscript denotes the vector component. The left hand side of (3.8) can be written as

$$\Delta \boldsymbol{v} \cdot \boldsymbol{f}_1 = \frac{f_1^{(1)}}{\hat{\rho}}\Delta\rho + (-2\bar{u}_1\bar{\beta}f_1^{(1)} + 2\bar{\beta}f_1^{(2)})\Delta u_1 + (-2\bar{u}_2\bar{\beta}f_1^{(1)} + 2\bar{\beta}f_1^{(3)})\Delta u_2$$

$$+(-2\bar{u}_3\bar{\beta}f_1^{(1)} + 2\bar{\beta}f_1^{(4)})\Delta u_3$$

$$+\left[\left(\frac{1}{(\gamma-1)\hat{\beta}} - \overline{|\boldsymbol{u}|^2}\right)f_1^{(1)} + 2\bar{u}_1 f_1^{(2)} + 2\bar{u}_2 f_1^{(3)} + 2\bar{u}_3 f_1^{(4)} - 2f_1^{(5)}\right.$$

$$\left.+2\bar{B}_1 f_1^{(6)} + 2\bar{B}_2 f_1^{(7)} + 2\bar{B}_3 f_1^{(8)}\right]\Delta\beta$$

$$+2\bar{\beta}f_1^{(6)}\Delta B_1 + 2\bar{\beta}f_1^{(7)}\Delta B_2 + 2\bar{\beta}f_1^{(8)}\Delta B_3$$

Similarly we write the differences $\Delta\mathcal{F}_1$ and $\Delta\phi$ as

$$\Delta\mathcal{F}_1 = \Delta(\rho u_1) + \Delta(\beta u_1|\boldsymbol{B}|^2)$$
$$= \bar{u}_1\Delta\rho + (\bar{\rho} + \bar{\beta}\ \overline{|\boldsymbol{B}|^2})\Delta u_1 + \bar{u}_1\overline{|\boldsymbol{B}|^2}\Delta\beta + 2\overline{\beta u_1}\ \bar{B}_1\Delta B_1 + 2\overline{\beta u_1}\ \bar{B}_2\Delta B_2 + 2\overline{\beta u_1}\ \bar{B}_3\Delta B_3$$

and

$$\Delta\phi = 2\Delta(\beta(\boldsymbol{u}\cdot\boldsymbol{B}))$$
$$= 2\bar{\beta}\ \bar{B}_1\Delta u_1 + 2\bar{\beta}\ \bar{B}_2\Delta u_2 + 2\bar{\beta}\ \bar{B}_3\Delta u_3 + 2(\bar{u}_1\ \bar{B}_1 + \bar{u}_2\ \bar{B}_2 + \bar{u}_3\ \bar{B}_3)\Delta\beta$$
$$+2\overline{\beta u_1}\Delta B_1 + 2\overline{\beta u_2}\Delta B_2 + 2\overline{\beta u_3}\Delta B_3$$

so that the right hand side of (3.8) can be written as

$$
\begin{aligned}
\Delta \mathcal{F}_1 - \overline{B}_1 \Delta \phi = \ & \overline{u}_1 \Delta \rho \\
& + (\overline{\rho} + \overline{\beta}\,\overline{|\boldsymbol{B}|^2} - 2\overline{\beta}\,\overline{B}_1 \overline{B}_1) \Delta u_1 \\
& - 2\overline{\beta}\,\overline{B}_1 \overline{B}_2 \Delta u_2 \\
& - 2\overline{\beta}\,\overline{B}_1 \overline{B}_3 \Delta u_3 \\
& + [\overline{u_1 |\boldsymbol{B}|^2} - 2(\overline{u}_1\,\overline{B}_1 + \overline{u}_2\,\overline{B}_2 + \overline{u}_3\,\overline{B}_3)\overline{B}_1] \Delta \beta \\
& + 2(\overline{\beta u_1}\,\overline{B}_2 - \overline{\beta u_2}\,\overline{B}_1) \Delta B_2 \\
& + 2(\overline{\beta u_1}\,\overline{B}_3 - \overline{\beta u_3}\,\overline{B}_1) \Delta B_3
\end{aligned}
$$

Equating the coefficients of $\Delta \rho$, Δu_1, Δu_2, Δu_3, ΔB_1, ΔB_2, ΔB_3 and $\Delta \beta$ on both sides of equation (3.8) in this order, we obtain the entropy conservative numerical fluxes as follows.

THEOREM 3.2. *The numerical fluxes given by*

$$
f_1^{(1)} = \hat{\rho} \overline{u}_1
$$

$$
f_1^{(2)} = \frac{\overline{\rho}}{2\overline{\beta}} + \overline{u}_1 f_1^{(1)} + \frac{1}{2}\overline{|\boldsymbol{B}|^2} - \overline{B}_1 \overline{B}_1
$$

$$
f_1^{(3)} = \overline{u}_2 f_1^{(1)} - \overline{B}_1 \overline{B}_2
$$

$$
f_1^{(4)} = \overline{u}_3 f_1^{(1)} - \overline{B}_1 \overline{B}_3
$$

$$
f_1^{(6)} = 0
$$

$$
f_1^{(7)} = \frac{1}{\overline{\beta}}(\overline{\beta u_1}\,\overline{B}_2 - \overline{\beta u_2}\,\overline{B}_1)
$$

$$
f_1^{(8)} = \frac{1}{\overline{\beta}}(\overline{\beta u_1}\,\overline{B}_3 - \overline{\beta u_3}\,\overline{B}_1)
$$

$$
f_1^{(5)} = \frac{1}{2}\left[\frac{1}{(\gamma-1)\hat{\beta}} - \overline{|\boldsymbol{u}|^2}\right] f_1^{(1)} + \overline{u}_1 f_1^{(2)} + \overline{u}_2 f_1^{(3)} + \overline{u}_3 f_1^{(4)}
$$

$$
\qquad + \overline{B}_1 f_1^{(6)} + \overline{B}_2 f_1^{(7)} + \overline{B}_3 f_1^{(8)} - \frac{1}{2}\overline{u_1 |\boldsymbol{B}|^2} + (\overline{u}_1 \overline{B}_1 + \overline{u}_2 \overline{B}_2 + \overline{u}_3 \overline{B}_3)\overline{B}_1
$$

satisfy equation (3.2).

Remark. We can check that the above numerical fluxes are consistent. Moreover, the condition that $f_1^{(6)} = 0$ which is the x component of the flux in the equation for B_1, comes out automatically in the above derivation. Similar expressions can be derived for the flux in the y direction which we do not list here. Note that since equation (3.2) is a scalar equation, there might be other choices for the flux that satisfy this equation. In fact in the case of Euler equations, several such fluxes are known, see [37, 21, 9]. In the rest of the paper, the above entropy conservative fluxes will be denoted by $\boldsymbol{f}^*$.

3.3. Entropy stable scheme. The finite volume scheme with the entropy conservative flux is not suitable for discontinuous solutions since entropy has to be generated at the shocks. Entropy generation at discontinuities amounts to replacing the equalities in (3.2), (3.3) with $\leq$ inequalities. In order to achieve this, we can add dissipative terms to the numerical flux. The form of the dissipative flux we choose involves the jump in the entropy variables at the cell interface which helps to obtain

an entropy inequality [37, 21, 15, 9]. We first state the general form of a numerical flux which achieves this property.

THEOREM 3.3. *Let* $\boldsymbol{f}^*_{1,i+\frac{1}{2},j}$, $\boldsymbol{f}^*_{2,i,j+\frac{1}{2}}$ *be entropy conservative fluxes satisfying (3.2), (3.3) respectively. Let* $D_{1,i+\frac{1}{2},j}$, $D_{2,i,j+\frac{1}{2}}$ *be symmetric positive definite matrices. Then the finite volume scheme (3.1) with numerical fluxes*
(3.9)
$$\boldsymbol{f}_{1,i+\frac{1}{2},j} = \boldsymbol{f}^*_{1,i+\frac{1}{2},j} - \frac{1}{2}D_{1,i+\frac{1}{2},j}\Delta\boldsymbol{v}_{i+\frac{1}{2},j}, \qquad \boldsymbol{f}_{2,i,j+\frac{1}{2}} = \boldsymbol{f}^*_{2,i,j+\frac{1}{2}} - \frac{1}{2}D_{2,i,j+\frac{1}{2}}\Delta\boldsymbol{v}_{i,j+\frac{1}{2}}$$

satisfies the cell entropy inequality

$$\frac{d}{dt}U(\boldsymbol{w}_{i,j}) + \frac{F_{1,i+\frac{1}{2},j} - F_{1,i-\frac{1}{2},j}}{\Delta x} + \frac{F_{2,i,j+\frac{1}{2}} - F_{2,i,j-\frac{1}{2}}}{\Delta y} \le 0$$

with the numerical entropy fluxes

$$F_{1,i+\frac{1}{2},j} = \overline{\boldsymbol{v}}_{i+\frac{1}{2},j} \cdot \boldsymbol{f}^*_{1,i+\frac{1}{2},j} + \overline{\phi}_{i+\frac{1}{2},j}\overline{B}_{1,i+\frac{1}{2},j} - \overline{\mathcal{F}}_{1,i+\frac{1}{2},j} + \frac{1}{2}\overline{\boldsymbol{v}}^\top_{i+\frac{1}{2},j}D_{1,i+\frac{1}{2},j}\Delta\boldsymbol{v}_{i+\frac{1}{2},j}$$

$$F_{2,i,j+\frac{1}{2}} = \overline{\boldsymbol{v}}_{i,j+\frac{1}{2}} \cdot \boldsymbol{f}^*_{2,i,j+\frac{1}{2}} + \overline{\phi}_{i,j+\frac{1}{2}}\overline{B}_{2,i,j+\frac{1}{2}} - \overline{\mathcal{F}}_{2,i,j+\frac{1}{2}} + \frac{1}{2}\overline{\boldsymbol{v}}^\top_{i,j+\frac{1}{2}}D_{2,i,j+\frac{1}{2}}\Delta\boldsymbol{v}_{i,j+\frac{1}{2}}$$

Proof: First of all, we can easily check that the above numerical entropy fluxes are consistent with the entropy flux as given in equation (2.13). Taking dot product of $\boldsymbol{v}_{i,j}$ with the finite volume scheme (3.1), a simple computation shows that we obtain

$$\frac{\mathrm{d}}{\mathrm{d}t}U(\boldsymbol{w}_{i,j}) + \frac{F_{1,i+\frac{1}{2},j} - F_{1,i-\frac{1}{2},j}}{\Delta x} + \frac{F_{2,i,j+\frac{1}{2}} - F_{2,i,j-\frac{1}{2}}}{\Delta y}$$
$$= -\frac{1}{2\Delta x}\left[\Delta\boldsymbol{v}^\top_{i+\frac{1}{2},j}D_{1,i+\frac{1}{2},j}\Delta\boldsymbol{v}_{i+\frac{1}{2},j} + \Delta\boldsymbol{v}^\top_{i-\frac{1}{2},j}D_{1,i-\frac{1}{2},j}\Delta\boldsymbol{v}_{i-\frac{1}{2},j}\right]$$
$$\quad -\frac{1}{2\Delta y}\left[\Delta\boldsymbol{v}^\top_{i,j+\frac{1}{2}}D_{2,i,j+\frac{1}{2}}\Delta\boldsymbol{v}_{i,j+\frac{1}{2}} + \Delta\boldsymbol{v}^\top_{i,j-\frac{1}{2}}D_{2,i,j-\frac{1}{2}}\Delta\boldsymbol{v}_{i,j-\frac{1}{2}}\right]$$
$$\le 0$$

where the numerical entropy fluxes are as defined in the theorem. The inequality is obtained because the dissipation matrices D_1, D_2 are positive definite.

3.4. Dissipation flux. The simplest choice for the dissipation matrices is a diagonal matrix $D_1 = \lambda I$ for some $\lambda > 0$. This amounts to adding a scalar dissipation which can lead to excessive amount of smearing of discontinuities since it does not distinguish between the various waves present in the solution. A more sophisticated approach is to add dissipation based on the eigenvectors like in the Roe scheme. Let us first write the modified MHD equations (2.8) in the conservation variables and in quasi-linear form as

$$\frac{\partial\boldsymbol{w}}{\partial t} + A_\alpha\frac{\partial\boldsymbol{w}}{\partial x_\alpha} = 0, \qquad A_\alpha = \boldsymbol{f}'_\alpha(\boldsymbol{w}) + \phi'(\boldsymbol{v})^\top B'_\alpha(\boldsymbol{w})$$

or in symmetric form using entropy variables

$$\tilde{A}_0\frac{\partial\boldsymbol{v}}{\partial t} + \tilde{A}_\alpha\frac{\partial\boldsymbol{v}}{\partial x_\alpha} = 0, \qquad \tilde{A}_0 = \boldsymbol{w}'(\boldsymbol{v}), \qquad \tilde{A}_\alpha = A_\alpha\tilde{A}_0$$

For any unit vector $\boldsymbol{n}$ define[†]

$$A(\boldsymbol{n}) = A_\alpha n_\alpha, \qquad \tilde{A}(\boldsymbol{n}) = \tilde{A}_\alpha n_\alpha = A(\boldsymbol{n})\tilde{A}_0$$

Note that $\tilde{A}_0$ is a right symmetrizer of the matrix $A(\boldsymbol{n})$. From the Eigenvector Scaling Theorem [4], it follows that there exist scaled eigenvectors of $A(\boldsymbol{n})$ such that

$$A(\boldsymbol{n}) = \tilde{R}(\boldsymbol{n})\Lambda(\boldsymbol{n})\tilde{R}^{-1}(\boldsymbol{n}), \qquad \tilde{A}_0 = \tilde{R}(\boldsymbol{n})\tilde{R}^\top(\boldsymbol{n}), \qquad \tilde{A}(\boldsymbol{n}) = \tilde{R}(\boldsymbol{n})\Lambda(\boldsymbol{n})\tilde{R}^\top(\boldsymbol{n})$$

By the definition of $\tilde{A}_0$ we have

$$d\boldsymbol{w} = \tilde{A}_0 d\boldsymbol{v} \qquad \text{and hence} \qquad \tilde{R}^{-1}(\boldsymbol{n})d\boldsymbol{w} = \tilde{R}^\top(\boldsymbol{n})d\boldsymbol{v}$$

The numerical flux of a Roe-type scheme [31, 16] across the face $(i+\frac{1}{2}, j)$ would be of the form

$$\boldsymbol{f}_{1,i+\frac{1}{2},j} = \frac{1}{2}(\boldsymbol{f}_{1,i,j} + \boldsymbol{f}_{1,i+1,j}) - \frac{1}{2}\tilde{R}(\boldsymbol{e}_1)|\Lambda(\boldsymbol{e}_1)|\tilde{R}(\boldsymbol{e}_1)^{-1}\Delta\boldsymbol{w}_{i+\frac{1}{2},j}, \qquad \boldsymbol{e}_1 = (1,0,0)$$

Using the transformation property between $\boldsymbol{w}$ to $\boldsymbol{v}$, we can write the dissipation flux in the above formula as

$$\frac{1}{2}\tilde{R}(\boldsymbol{e}_1)|\Lambda(\boldsymbol{e}_1)|\tilde{R}(\boldsymbol{e}_1)^{-1}\Delta\boldsymbol{w}_{i+\frac{1}{2},j} \approx \frac{1}{2}\tilde{R}(\boldsymbol{e}_1)|\Lambda(\boldsymbol{e}_1)|\tilde{R}(\boldsymbol{e}_1)^\top\Delta\boldsymbol{v}_{i+\frac{1}{2},j}$$

Hence the dissipation matrices can be taken to be

$$(3.10) \qquad D_{1,i+\frac{1}{2},j} = \tilde{R}_{i+\frac{1}{2},j}|\Lambda_{i+\frac{1}{2},j}|\tilde{R}^\top_{i+\frac{1}{2},j}, \qquad D_{2,i,j+\frac{1}{2}} = \tilde{R}_{i,j+\frac{1}{2}}|\Lambda_{i,j+\frac{1}{2}}|\tilde{R}^\top_{i,j+\frac{1}{2}}$$

where the eigenvectors and eigenvalues are computed at some average state corresponding to the interface. The eight eigenvalues Λ and the corresponding eigenvectors were derived in [4] and are given in the Appendix.

3.5. High resolution scheme. The scheme (3.1), (3.9), (3.10) is first order accurate in space due to the presence of terms like $\Delta\boldsymbol{v}_{i+\frac{1}{2},j}$ which are $O(\Delta x)$ for smooth functions. Higher order accurate schemes are obtained by a more accurate computation of the jump at the cell faces. Define the set of primitive variables $\boldsymbol{q} = [\rho, \boldsymbol{u}, p, \boldsymbol{B}]^\top$ which we will use to express some of the quantities since they have simple dependencies. The numerical flux of the first order scheme in the x_1 direction can be written as

$$\boldsymbol{f}_{1,i+\frac{1}{2},j} = \boldsymbol{f}_1^*(\boldsymbol{q}_{i,j}, \boldsymbol{q}_{i+1,j}) - \frac{1}{2}D_1(\boldsymbol{q}_{i,j}, \boldsymbol{q}_{i+1,j})(\boldsymbol{v}_{i+1,j} - \boldsymbol{v}_{i,j})$$

The dissipation matrix D_1 is evaluated at an average state of the interface $(i+\frac{1}{2}, j)$ which we indicate by its dependance on the two states $\boldsymbol{q}_{i,j}$ and $\boldsymbol{q}_{i+1,j}$. For the higher order scheme, the numerical flux is given by

$$\boldsymbol{f}_{1,i+\frac{1}{2},j} = \boldsymbol{f}_1^*(\boldsymbol{q}_{i,j}, \boldsymbol{q}_{i+1,j}) - \frac{1}{2}D_1(\boldsymbol{q}_{i,j}, \boldsymbol{q}_{i+1,j})(\boldsymbol{v}^R_{i+\frac{1}{2},j} - \boldsymbol{v}^L_{i+\frac{1}{2},j})$$

where $\boldsymbol{v}^R_{i+\frac{1}{2},j}$, $\boldsymbol{v}^L_{i+\frac{1}{2},j}$ are obtained by a reconstruction process. For this purpose let us define the minmod function

$$\mathcal{M}(a,b) = \begin{cases} s\min(|a|, |b|) & \text{if} \quad s = \text{sign}(a) = \text{sign}(b) \\ 0 & \text{otherwise} \end{cases}$$

[†]These quantities depend on the state $\boldsymbol{w}$ but we do not show the explicit dependance to keep the notation simple.

i.e., this function selects the smallest value in absolute terms. For each interface $(i + \frac{1}{2}, j)$, let us define a new set of variables

$$z_{k,j} = \tilde{R}_{i+\frac{1}{2},j}^\top v_{k,j}, \qquad k = i-1, i, i+1, i+2 \qquad \tilde{R}_{i+\frac{1}{2},j} = \tilde{R}(e_1, q_{i,j}, q_{i+1,j})$$

We reconstruct the variable z using the minmod function and compute v by inverting the above relationship, i.e.,

$$z_{i+\frac{1}{2},j}^L = z_{i,j} + \frac{1}{2}\mathcal{M}\left(z_{i,j} - z_{i-1,j}, z_{i+1,j} - z_{i,j}\right)$$

$$z_{i+\frac{1}{2},j}^R = z_{i+1,j} - \frac{1}{2}\mathcal{M}\left(z_{i+1,j} - z_{i,j}, z_{i+2,j} - z_{i+1,j}\right)$$

and

$$v_{i+\frac{1}{2},j}^L = (\tilde{R}_{i+\frac{1}{2},j}^\top)^{-1} z_{i+\frac{1}{2},j}^L, \qquad v_{i+\frac{1}{2},j}^R = (\tilde{R}_{i+\frac{1}{2},j}^\top)^{-1} z_{i+\frac{1}{2},j}^R$$

Note that this reconstruction must be performed at each interface since the variable z is defined at a particular interface by the above formula. We point out that the entropy conservative flux f_1^* is computed using the solution at the cell centers and the reconstructed values are used only in the jump terms in the dissipative flux. In practice it is not necessary to invert the eigenvector matrix and we compute the higher order numerical flux as

$$f_{1,i+\frac{1}{2},j} = f_1^*(q_{i,j}, q_{i+1,j}) - \frac{1}{2}\tilde{R}_{i+\frac{1}{2},j}|\Lambda_{i+\frac{1}{2},j}|(z_{i+\frac{1}{2},j}^R - z_{i+\frac{1}{2},j}^L)$$

A similar procedure is performed to compute the flux in the y direction. With this reconstruction procedure, the entropy stability of the semi-discrete finite volume scheme can be below. For convenience let us define

$$[\![\cdot]\!]_{i+\frac{1}{2},j} = (\cdot)_{i+\frac{1}{2},j}^R - (\cdot)_{i+\frac{1}{2},j}^L, \qquad [\![\cdot]\!]_{i,j+\frac{1}{2}} = (\cdot)_{i,j+\frac{1}{2}}^R - (\cdot)_{i,j+\frac{1}{2}}^L$$

THEOREM 3.4. *Let $f_{1,i+\frac{1}{2},j}^*$, $f_{2,i,j+\frac{1}{2}}^*$ be entropy conservative fluxes satisfying (3.2), (3.3) respectively, and $D_{1,i+\frac{1}{2},j}$, $D_{2,i,j+\frac{1}{2}}$ be symmetric positive definite matrices given by (3.10). Then the finite volume scheme (3.1) with numerical fluxes (3.11)*

$$f_{1,i+\frac{1}{2},j} = f_{1,i+\frac{1}{2},j}^* - \frac{1}{2}D_{1,i+\frac{1}{2},j}[\![v]\!]_{i+\frac{1}{2},j}, \qquad f_{2,i,j+\frac{1}{2}} = f_{2,i,j+\frac{1}{2}}^* - \frac{1}{2}D_{2,i,j+\frac{1}{2}}[\![v]\!]_{i,j+\frac{1}{2}}$$

satisfies the cell entropy inequality

$$\frac{d}{dt}U(w_{i,j}) + \frac{F_{1,i+\frac{1}{2},j} - F_{1,i-\frac{1}{2},j}}{\Delta x} + \frac{F_{2,i,j+\frac{1}{2}} - F_{2,i,j-\frac{1}{2}}}{\Delta y} \leq 0$$

with the numerical entropy fluxes

$$F_{1,i+\frac{1}{2},j} = \overline{v}_{i+\frac{1}{2},j} \cdot f_{1,i+\frac{1}{2},j}^* + \overline{\phi}_{i+\frac{1}{2},j}\overline{B}_{1,i+\frac{1}{2},j} - \overline{\mathcal{F}}_{1,i+\frac{1}{2},j} + \frac{1}{2}\overline{v}_{i+\frac{1}{2},j}^\top D_{1,i+\frac{1}{2},j}[\![v]\!]_{i+\frac{1}{2},j}$$

$$F_{2,i,j+\frac{1}{2}} = \overline{v}_{i,j+\frac{1}{2}} \cdot f_{2,i,j+\frac{1}{2}}^* + \overline{\phi}_{i,j+\frac{1}{2}}\overline{B}_{2,i,j+\frac{1}{2}} - \overline{\mathcal{F}}_{2,i,j+\frac{1}{2}} + \frac{1}{2}\overline{v}_{i,j+\frac{1}{2}}^\top D_{2,i,j+\frac{1}{2}}[\![v]\!]_{i,j+\frac{1}{2}}$$

<u>Proof</u>: If $\boldsymbol{w}_{i,j} = \boldsymbol{w}_{i+1,j}$ then $\boldsymbol{z}^L_{i+\frac{1}{2},j} = \boldsymbol{z}^R_{i+\frac{1}{2},j}$ and hence $\boldsymbol{v}^L_{i+\frac{1}{2},j} = \boldsymbol{v}^R_{i+\frac{1}{2},j}$. The numerical entropy flux $F_{1,i+\frac{1}{2},j}$ is consistent with the entropy flux as given in equation (2.13). Similarly we see that $F_{2,i,j+\frac{1}{2}}$ is also consistent. Taking dot product of $\boldsymbol{v}_{i,j}$ with the finite volume scheme (3.1), a simple computation shows that we obtain

$$
\frac{\mathrm{d}}{\mathrm{d}t}U(\boldsymbol{w}_{i,j}) + \frac{F_{1,i+\frac{1}{2},j} - F_{1,i-\frac{1}{2},j}}{\Delta x} + \frac{F_{2,i,j+\frac{1}{2}} - F_{2,i,j-\frac{1}{2}}}{\Delta y}
$$

$$
= -\frac{1}{2\Delta x}\left[\Delta\boldsymbol{v}^\top_{i+\frac{1}{2},j}D_{1,i+\frac{1}{2},j}[\![\boldsymbol{v}]\!]_{i+\frac{1}{2},j} + \Delta\boldsymbol{v}^\top_{i-\frac{1}{2},j}D_{1,i-\frac{1}{2},j}[\![\boldsymbol{v}]\!]_{i-\frac{1}{2},j}\right]
$$

$$
-\frac{1}{2\Delta y}\left[\Delta\boldsymbol{v}^\top_{i,j+\frac{1}{2}}D_{2,i,j+\frac{1}{2}}[\![\boldsymbol{v}]\!]_{i,j+\frac{1}{2}} + \Delta\boldsymbol{v}^\top_{i,j-\frac{1}{2}}D_{2,i,j-\frac{1}{2}}[\![\boldsymbol{v}]\!]_{i,j-\frac{1}{2}}\right]
$$

$$
= -\frac{1}{2\Delta x}\left[\Delta\boldsymbol{z}^\top_{i+\frac{1}{2},j}|\Lambda_{i+\frac{1}{2},j}|[\![\boldsymbol{z}]\!]_{i+\frac{1}{2},j} + \Delta\boldsymbol{z}^\top_{i-\frac{1}{2},j}|\Lambda_{i-\frac{1}{2},j}|[\![\boldsymbol{z}]\!]_{i-\frac{1}{2},j}\right]
$$

$$
-\frac{1}{2\Delta y}\left[\Delta\boldsymbol{z}^\top_{i,j+\frac{1}{2}}|\Lambda_{i,j+\frac{1}{2}}|[\![\boldsymbol{z}]\!]_{i,j+\frac{1}{2}} + \Delta\boldsymbol{z}^\top_{i,j-\frac{1}{2}}|\Lambda_{i,j-\frac{1}{2}}|[\![\boldsymbol{z}]\!]_{i,j-\frac{1}{2}}\right]
$$

$$
\leq 0
$$

where the numerical entropy fluxes are as defined in the theorem. The last inequality is obtained because the reconstruction based on the minmod function satisfies the sign property, i.e.,

$$
\mathrm{sign}([\![\boldsymbol{z}]\!]_{i+\frac{1}{2},j}) = \mathrm{sign}(\Delta\boldsymbol{z}_{i+\frac{1}{2},j}), \qquad \text{etc.}
$$

for each component of $\boldsymbol{z}$. This proves the desired result.

Remark. The crucial property in the above proof was the sign property of the reconstruction scheme. Any other reconstruction scheme for the $\boldsymbol{z}$ variables that satisfies this property can also be used, e.g., the ENO-2 scheme. In fact, the extension to arbitrarily higher orders of accuracy is possible using an ENO approach for which the sign property has been shown in [15].

4. Numerical results. In this section, we present numerical results on some standard two dimensional MHD test cases to illustrate the robustness of the proposed scheme in computing discontinuous flows. The semi-discrete equations (3.1) are integrated in time using a 3-stage, 3'rd order accurate strong stability preserving Runge-Kutta scheme [35]. The time step is chosen based on the following CFL condition

$$
\Delta t = \mathrm{cfl} \cdot \min_{i,j}\left(\frac{|(u_1)_{i,j}| + (c_{f,1})_{i,j}}{\Delta x} + \frac{|(u_2)_{i,j}| + (c_{f,2})_{i,j}}{\Delta y}\right)^{-1}, \qquad 0 < \mathrm{cfl} \leq 1
$$

where $c_{f,1}$ and $c_{f,2}$ are the fast speeds in the x_1 and x_2 directions, see Appendix. We use a cfl number of 0.9 in all the test cases.

4.1. Orszag-Tang vortex. This test case was originally proposed in [29] and is widely used to test MHD schemes. The set of parameters we use for the test case are similar to [39]. The computational domain is taken to be $[0,1] \times [0,1]$ with periodic boundary conditions on all sides, the constant $\gamma = \frac{5}{3}$ and initial condition is given by

$$
\rho = \frac{25}{36\pi}, \qquad \boldsymbol{u} = (-\sin(2\pi y),\ \sin(2\pi x),\ 0), \qquad p = \frac{5}{12\pi}
$$

$$
\boldsymbol{B} = \frac{1}{\sqrt{4\pi}}(-\sin(2\pi y),\ \sin(4\pi x),\ 0)
$$

The smooth initial condition evolves to a more complex flow with many discontinuities and eventually into turbulence. The solution at time $t = 0.5$ is shown in figure (1) on grids of sizes 128×128, 256×256, 512×512 and 1024×1024. We find that the computations are stable on all the meshes, including on the very fine mesh, which shows the robustness of the scheme. The large scale structures are resolved on all meshes, but we see better resolution of the many small scale features with mesh refinement. To test the importance of the source terms, we performed a computation by switching off the source terms but retaining the rest of the scheme. The computations however break down after some time due to loss of positivity of density/pressure, indicating the important of the source terms and the resulting entropy stability. The entropy stability of the scheme is established only at the semi-discrete level. With explicit time discretization by a Runge-Kutta scheme, we cannot prove the entropy stability. We compute the total entropy $\sum_{i,j} U(\boldsymbol{w}_{i,j}^n) \Delta x \Delta y$ which in principle should decrease with time if the scheme is entropy stable. This quantity is plotted in figure (2a) and we observe that the total entropy does not increase with time. Since the solution is smooth in the initial times, the entropy is constant and then it starts to decrease when discontinuities start to form.

4.2. Rotor test. This test case was first proposed in [3] but we use the version given in [39], where it is refered to as the *first rotor problem*. The computational domain is $[0, 1] \times [0, 1]$ with periodic boundary conditions on all sides, the constant $\gamma = \frac{5}{3}$ and the initial condition is given as follows. For $r < r_0$,

$$\rho = 10, \qquad (u_1, u_2) = \frac{u_0}{r_0}(-(y - 1/2),\ (x - 1/2))$$

and for $r_0 < r < r_1$

$$\rho = 1 + 9f, \qquad (u_1, u_2) = \frac{fu_0}{r}(-(y - 1/2),\ (x - 1/2)), \qquad f = \frac{r_1 - r}{r_1 - r_0}$$

and for $r > r_1$

$$\rho = 1, \qquad (u_1, u_2) = (0, 0)$$

with $r_0 = 0.1$, $r_1 = 0.115$ and $u_0 = 2$. The rest of the quantities are constant and given by

$$u_3 = 0, \qquad p = 1, \qquad \boldsymbol{B} = \frac{5}{4\pi}(1,\ 0,\ 0)$$

The computations are performed on grids of sizes 128×128, 256×256, 512×512 and 1024×1024. The Mach number contours are shown in figure (3). The circularly rotating velocity field in the central portion is captured well in all the grids without any distortion. Toth [39] reports that some dimensionally split schemes might lead to loss of positivity which was not a problem with our unsplit scheme. However if we do not add the source terms, then the computations were unstable due to loss of positivity. The total entropy is shown in figure (2b) and we again observe a monotonic decay which indicates that the fully discrete scheme is also entropy stable.

4.3. Smooth Alfvén waves. This test case is taken from [39] and consists of a circularly polarized Alfvén wave which propagates at an angle of $\alpha = 30^o$. The domain is taken to be the rectangle defined by $0 \leq x \leq 1/\cos\alpha$ and $0 \leq y \leq 1/\sin\alpha$
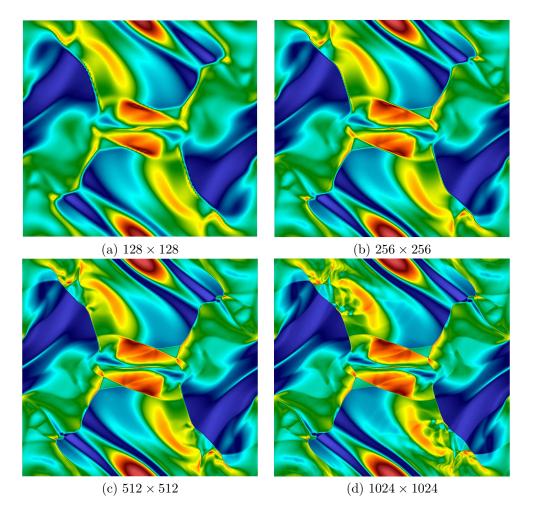
(a) 128×128 (b) 256×256

(c) 512×512 (d) 1024×1024

FIG. 1. *Density at $t = 0.5$ for Orszag-Tang test case on different meshes. The density range is 0.09 to 0.48*

(a)   (b)

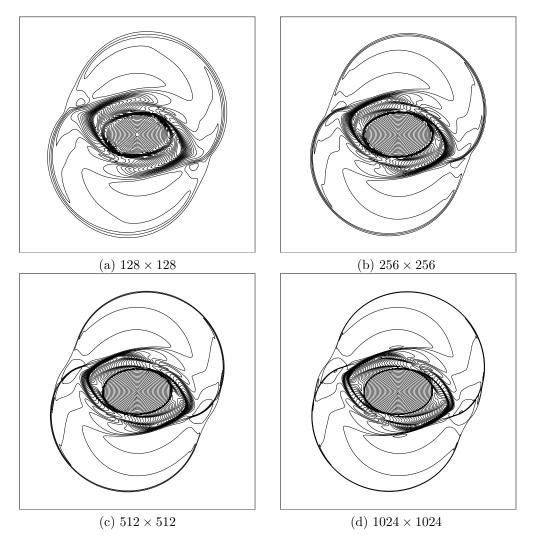FIG. 2. *Evolution of total entropy with time: (a) Orszag-Tang test (b) Rotor test*

(a) 128×128

(b) 256×256

(c) 512×512

(d) 1024×1024

Fig. 3. *Mach contours for rotor test case at time $t = 0.15$ on different meshes. 30 contours between 0 and 4.2 are shown.*

with periodic boundary conditions on all sides. The constant $\gamma = \frac{5}{3}$ and the initial condition is given as follows.

$$\rho = 1, \qquad \boldsymbol{u} = v_\perp(-\sin\alpha, \cos\alpha, 0), \qquad p = 0.1$$

$$B_1 = B_{||} \cos\alpha - B_\perp \sin\alpha, \qquad B_2 = B_{||} \sin\alpha + B_\perp \cos\alpha, \qquad B_3 = u_3$$

$$B_{||} = 1, \qquad B_\perp = v_\perp = 0.1\sin(2\pi x_{||}), \qquad x_{||} = x\cos\alpha + y\sin\alpha$$

Due to periodicity the solution returns to its initial state after a time of $t = 1$ units which is the period of the solution. Figure (4) shows $B_\perp = B_2\cos\alpha - B_1\sin\alpha$ at time $t = 5$ on meshes of sizes 32×32, 64×64 and 128×128. In (4a) we show the results using the entropy stable scheme and we observe that the solutions converge
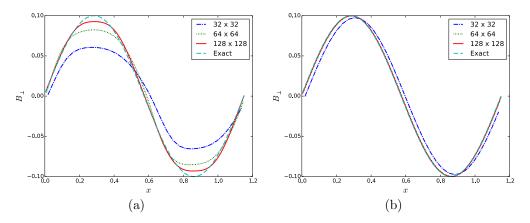
FIG. 4. *Plot of $B_\perp$ along $y = 0$ for the circularly polarized Alfvén wave at $t = 5$. (a) Entropy stable scheme, (b) MUSCL-type reconstruction*

with grid refinement. However there is loss of accuracy at the smooth extrema which is a general problem with limiters. We show the same results in (4b) where a MUSCL-type reconstruction is used without any limiting and we observe very good accuracy including at the extrema.

4.4. Rotated shock tube problem. This test case is taken from [34] and consists of a shock tube problem which is oblique to the Cartesian mesh. The shock propagates at an angle of $\alpha = 45^o$ and the initial left and right data in terms of the primitive variables $(\rho, \boldsymbol{u}, p, \boldsymbol{B})$ are given by $(1, 10, 0, 0, 20, 5/\sqrt{4\pi}, 5/\sqrt{4\pi}, 0)$ and $(1, -10, 0, 0, 1, 5/\sqrt{4\pi}, 5/\sqrt{4\pi}, 0)$ respectively. The initial discontinuity is along the line $x + y = 1/2$ and we set the initial conditions by performing an averaging. The mesh is Cartesian with $\Delta x = \Delta y$; we use 10 cells in the y direction and 256 or 512 cells in the x direction. Since the shock is oblique we used shifted periodic boundary conditions on the top and bottom of the domain as explained in [39]. The solution is computed until the time $t = 0.08 \cos(\alpha)$ and slices along x axis are shown in figure (5). These may be compared with the solutions from [34] except that they plot the slice along the line $x = y$. The parallel component of magnetic field $B_\parallel$ should be constant for this problem but this is not maintained by the scheme due to its lack of conservation property, also see similar test case in [39] and the results from a non-conservative 8-wave scheme. The other quantities shown have correct behaviour (compare with [34]) except for oscillations near the shocks, which could again be a consequence of non-conservative nature of the scheme. If we switch off the source terms in the scheme and compute the solution, then we obtain a better solution for $B_\parallel$, while other quantities do not change significantly.

5. Summary and conclusions. We have constructed an entropy stable finite volume scheme for the equations of ideal compressible MHD. This is achieved by starting from Godunov's symmetrization of MHD equations for which an entropy conservative scheme is first constructed. A characterization is given on the numerical flux which leads to entropy conservation property. We have also derived a numerical flux with simple expressions which satisfies this property. This scheme is made entropy stable by adding suitable dissipation terms based on entropy variables. Then a high resolution scheme based on a reconstruction process applied to scaled entropy variables is constructed which is also entropy stable. The new scheme is applied to
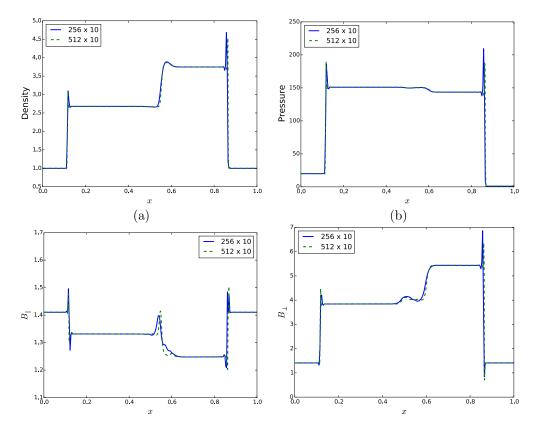
FIG. 5. *Results for the rotated shock tube problem on two different meshes. (a) Density, (b) Pressure, (c) $B_\| = (B_1 + B_2)/\sqrt{2}$, (d) $B_\perp = (-B_1 + B_2)/\sqrt{2}$*

some standard MHD test cases which show its robustness in computing discontinuous solutions even on very fine meshes. The additional source terms introduced by Godunov (and later by Powell) which are necessary for symmetrization of the equations and for obtaining entropy stability, are found to be also crucial to maintain numerical stability since the computations fail in some test cases due to loss of positivity of density/pressure if we do not add these terms. While the fully discrete scheme with explicit Runge-Kutta time stepping is not provably entropy stable, the numerical tests show that the entropy condition is satisfied under time discretization and a CFL condition. However, the lack of conservation property can lead to wrong solutions in some cases as seen in the rotated shock tube problem. Thus in the finite volume setting, there is a conflict between entropy stability which requires the source terms, and conservation property which is lost due to the source terms. As discussed in the introduction, the proposed entropy stable fluxes can be used in a discontinuous galerkin scheme to obtain a conservative and entropy stable scheme which is part of our ongoing work.

Appendix A. Entropy scaled eigenvectors for ideal MHD.

In this section we list the eigenvectors and eigenvalues of the symmetrized equations (2.8) as derived by Barth [4]. Define the vector $\boldsymbol{b} = \frac{\boldsymbol{B}}{\sqrt{\rho}}$ and the fast and slow speeds by

$$c_{f,s}^2 = \frac{1}{2}(a^2 + |\boldsymbol{b}|^2) \pm \frac{1}{2}\sqrt{(a^2 + |\boldsymbol{b}|^2)^2 - 4a^2(\boldsymbol{b} \cdot \boldsymbol{n})^2}$$

We also define the following quantities which are useful to simplify the expressions

$$\alpha_f^2 = \frac{a^2 - c_s^2}{c_f^2 - c_s^2}, \qquad \alpha_s^2 = \frac{c_f^2 - a^2}{c_f^2 - c_s^2}$$

Let $\boldsymbol{n}^\perp$ a unit vector orthogonal to $\boldsymbol{n}$ and lying in the plane spanned by $\boldsymbol{n}$ and $\boldsymbol{b}$, i.e.,

$$\boldsymbol{n}^\perp \cdot \boldsymbol{n} = 0, \qquad |\boldsymbol{n}^\perp| = 1, \qquad \boldsymbol{n}^\perp \in \mathrm{span}\{\boldsymbol{n}, \boldsymbol{b}\}$$

The eigenvectors with respect to the primitive variables $(\rho, \boldsymbol{u}, p, \boldsymbol{B})$ are given below together with the corresponding eigenvalues. To obtain the eigenvectors corresponding to the conserved variables, we have to multiply the following vectors with the Jacobian of the transformation.

Entropy and divergence wave: $\lambda_1 = \lambda_2 = \boldsymbol{u} \cdot \boldsymbol{n}$

$$\tilde{r}_1 = \sqrt{\frac{\gamma - 1}{\gamma}} \begin{bmatrix} \sqrt{\rho} \\ \boldsymbol{0} \\ 0 \\ \boldsymbol{0} \end{bmatrix}, \qquad \tilde{r}_2 = \frac{1}{\sqrt{\gamma}} \begin{bmatrix} 0 \\ \boldsymbol{0} \\ 0 \\ a\boldsymbol{n} \end{bmatrix}$$

Alfvén waves: $\lambda_a^\pm = \boldsymbol{u} \cdot \boldsymbol{n} \pm \boldsymbol{b} \cdot \boldsymbol{n}$

$$\tilde{r}_a^\pm = \frac{1}{\sqrt{2\gamma}} \begin{bmatrix} 0 \\ \mp \frac{a}{\sqrt{\rho}}(\boldsymbol{n}^\perp \times \boldsymbol{n}) \\ 0 \\ a(\boldsymbol{n}^\perp \times \boldsymbol{n}) \end{bmatrix}$$

Fast magneto-acoustic waves: $\lambda_f^\pm = \boldsymbol{u} \cdot \boldsymbol{n} \pm c_f$

$$\tilde{r}_f^\pm = \frac{1}{\sqrt{2\gamma}} \begin{bmatrix} \alpha_f \sqrt{\rho} \\ \pm \frac{1}{\sqrt{\rho}c_f}[\alpha_f a^2 \boldsymbol{n} + \alpha_s a\{(\boldsymbol{b} \cdot \boldsymbol{n}^\perp)\boldsymbol{n} - (\boldsymbol{b} \cdot \boldsymbol{n})\boldsymbol{n}^\perp\}] \\ \alpha_f \sqrt{\rho} a^2 \\ \alpha_s a \boldsymbol{n}^\perp \end{bmatrix}$$

Slow magneto-acoustic waves: $\lambda_s^\pm = \boldsymbol{u} \cdot \boldsymbol{n} \pm c_s$

$$\tilde{r}_s^\pm = \frac{1}{\sqrt{2\gamma}} \begin{bmatrix} \alpha_s \sqrt{\rho} \\ \pm \frac{\mathrm{sign}(\boldsymbol{b} \cdot \boldsymbol{n})}{\sqrt{\rho}c_f}[\alpha_s a(\boldsymbol{b} \cdot \boldsymbol{n})\boldsymbol{n} + \alpha_f c_f^2 \boldsymbol{n}^\perp] \\ \alpha_s \sqrt{\rho} a^2 \\ -\alpha_f a \boldsymbol{n}^\perp \end{bmatrix}$$

REFERENCES

[1] D. S. BALSARA, *Divergence-free reconstruction of magnetic fields and {WENO} schemes for magnetohydrodynamics*, Journal of Computational Physics, 228 (2009), pp. 5040 – 5056.

[2] D. S. BALSARA, T. RUMPF, M. DUMBSER, AND C.-D. MUNZ, *Efficient, high accuracy ADER-WENO schemes for hydrodynamics and divergence-free magnetohydrodynamics*, J. Comput. Phys., 228 (2009), pp. 2480–2516.

[3] D. S. BALSARA AND D. S. SPICER, *A staggered mesh algorithm using high order Godunov fluxes to ensure solenoidal magnetic fields in magnetohydrodynamic simulations*, Journal of Computational Physics, 149 (1999), pp. 270 – 292.

[4] T. BARTH, *Numerical methods for gasdynamic systems on unstructured grids*, in An introduction to recent developments in theory and numerics for conservation laws, Kroner, Ohlberger, and Rohde, eds., vol. 5 of Lecture Notes in Computational Science and Engineering, Springer-Verlag, 1998, pp. 198–285.

[5] T. J. BARTH, *On the role of involutions in the discontinuous Galerkin discretization of Maxwell and magnetohydrodynamic systems*, in IMA Volume on Compatible Spatial Discretizations, vol. 142, Springer-Verlag, 2005.

[6] F. BOUCHUT, C. KLINGENBERG, AND K. WAAGAN, *A multiwave approximate riemann solver for ideal mhd based on relaxation. i: Theoretical framework*, Numer. Math., 108 (2007), pp. 7–42.

[7] J. BRACKBILL AND D. BARNES, *The effect of nonzero ∇·b on the numerical solution of the magnetohydrodynamic equations*, Journal of Computational Physics, 35 (1980), pp. 426 – 430.

[8] M. BRIO AND C. C. WU, *An upwind differencing scheme for the equations of ideal magnetohydrodynamics*, J. Comput. Phys., 75 (1988), pp. 400–422.

[9] P. CHANDRASHEKAR, *Kinetic energy preserving and entropy stable finite volume schemes for compressible Euler and Navier-Stokes equations*, Commun. Comput. Phys., 14 (2013).

[10] W. DAI AND P. R. WOODWARD, *An approximate riemann solver for ideal magnetohydrodynamics*, J. Comput. Phys., 111 (1994), pp. 354–372.

[11] A. DEDNER, F. KEMM, D. KRÖNER, C.-D. MUNZ, T. SCHNITZER, AND M. WESENBERG, *Hyperbolic divergence cleaning for the MHD equations*, Journal of Computational Physics, 175 (2002), pp. 645 – 673.

[12] C. R. EVANS AND J. F. HAWLEY, *Simulation of magnetohydrodynamic flows - A constrained transport method*, Astrophysical Journal, 332 (1988), pp. 659–677.

[13] L. C. EVANS, *Partial Differential Equations*, Graduate Studies in Mathematics, American Mathematical Society, 2010.

[14] M. FEY AND M. TORRILHON, *A constrained transport upwind scheme for divergence-free advection*, in Hyperbolic Problems: Theory, Numerics, Applications, T. Hou and E. Tadmor, eds., Springer Berlin Heidelberg, 2003, pp. 529–538.

[15] U. FJORDHOLM, S. MISHRA, AND E. TADMOR, *Arbitrarily high-order accurate entropy stable essentially nonoscillatory schemes for systems of conservation laws*, SIAM Journal on Numerical Analysis, 50 (2012), pp. 544–573.

[16] T. GALLOUET AND J. M. MASELLA, *On a rough Godunov scheme*, Compte Rendus, Paris, Series I, 323 (1996), pp. 77–84.

[17] E. GODLEWSKI AND P. RAVIART, *Numerical Approximation of Hyperbolic Systems of Conservation Laws*, Springer, 1996.

[18] S. K. GODUNOV, *The symmetric form of magnetohydrodynamics equation*, Num. Meth. Mech. Cont. Media, 34 (1972), pp. 1–26.

[19] K. F. GURSKI, *An HLLC-type approximate Riemann solver for ideal magnetohydrodynamics*, SIAM Journal on Scientific Computing, 25 (2004), pp. 2165–2187.

[20] C. HELZEL, J. A. ROSSMANITH, AND B. TAETZ, *An unstaggered constrained transport method for the 3d ideal magnetohydrodynamic equations*, J. Comput. Phys., 230 (2011), pp. 3803–3829.

[21] F. ISMAIL AND P. L. ROE, *Affordable, entropy-consistent Euler flux functions II: Entropy production at shocks*, J. Comput. Phys., 228 (2009), pp. 5410–5436.

[22] P. JANHUNEN, *A positive conservative method for magnetohydrodynamics based on hll and roe methods*, J. Comput. Phys., 160 (2000), pp. 649–661.

[23] C. KLINGENBERG AND K. WAAGAN, *Relaxation solvers for ideal MHD equations - A review*, Acta Mathematica Scientia, 30B (2010), pp. 621–632.

[24] P. LEFLOCH, J. MERCIER, AND C. ROHDE, *Fully discrete, entropy conservative schemes of arbitraryorder*, SIAM Journal on Numerical Analysis, 40 (2002), pp. 1968–1992.

[25] F. LI AND C.-W. SHU, *Locally divergence-free discontinuous galerkin methods for mhd equations*, Journal of Scientific Computing, 22-23 (2005), pp. 413–442.

[26] F. LI AND L. XU, *Arbitrary order exactly divergence-free central discontinuous galerkin methods*

for ideal mhd equations, J. Comput. Phys., 231 (2012), pp. 2655–2675.

[27] E. LODLEWSKI AND P.-A. RAVIART, *Hyperbolic systems of conservation laws*, Ellipses, 1991.

[28] P. LONDRILLO AND L. D. ZANNA, *High-order upwind schemes for multidimensional magneto-hydrodynamics*, The Astrophysical Journal, 530 (2000), p. 508.

[29] S. A. ORSZAG AND C.-M. TANG, *Small-scale structure of two-dimensional magnetohydrodynamic turbulence*, Journal of Fluid Mechanics, 90 (1979), pp. 129–143.

[30] K. POWELL, *An approximate Riemann solver for magnetohydrodynamics (that works in more than one dimension)*, Tech. Rep. 94-24, ICASE, NASA Langley, 1994.

[31] P. L. ROE, *Approximate Riemann solvers, parameter vectors, and difference schemes*, Journal of Computational Physics, 43 (1981), pp. 357 – 372.

[32] ———, *Affordable, entropy consistent flux functions*, in Eleventh International Conference on Hyperbolic Problems: Theory, Numerics and Applications, Lyon, 2006.

[33] J. A. ROSSMANITH, *An unstaggered, high-resolution constrained transport method for magnetohydrodynamic flows*, SIAM J. Sci. Comput., 28 (2006), pp. 1766–1797.

[34] D. RYU, F. MINIATI, T. W. JONES, AND A. FRANK, *A divergence-free upwind code for multidimensional magnetohydrodynamic flows*, Astrophysical Journal, 509 (1998).

[35] C.-W. SHU AND S. OSHER, *Efficient implementation of essentially non-oscillatory shock-capturing schemes*, Journal of Computational Physics, 77 (1988), pp. 439 – 471.

[36] E. TADMOR, *The numerical viscosity of entropy stable schemes for systems of conservation laws. I*, Mathematics of Computation, 49 (1987), pp. pp. 91–103.

[37] E. TADMOR, *Entropy stability theory for difference approximations of nonlinear conservation laws and related time-dependent problems*, Acta Numerica, (2004), pp. 451–512.

[38] Q. TANG, A. CHRISTLIEB, Y. GUCLU, AND J. ROSSMANITH, *Finite difference weighted essentially non-oscillatory schemes with constrained transport for 2d ideal magnetohydrodynamics*, in Plasma Science (ICOPS), 2013 Abstracts IEEE International Conference on, June 2013, pp. 1–1.

[39] G. TOTH, *The $\nabla \cdot B = 0$ constraint in shock-capturing magnetohydrodynamics codes*, Journal of Computational Physics, 161 (2000), pp. 605 – 652.